LES OF TRANSIENTS IN THE FRANCIS-99 WATER TURBINE MODEL

Jonathan Fahlbeck[1], Ludvig Uppström[2], Eric Lillberg[3], Håkan Nilsson[4]
[1]MSc student, Chalmers University of Technology, Mechanics and Martime Sciences,
jonathan.fahlbeck@outlook.com
[2]MSc student, Chalmers University of Technology, Mechanics and Martime Sciences,
ludvig.uppstrom@gmail.com
[3]Vattenfall AB Research and Development, *eric.lillberg@vattenfall.com*
[4]Chalmers University of Technology, Mechanics and Maritime Sciences, *hakan.nilsson@chalmers.se*

Due to the new intermittent electric energy sources, hydropower is forced to run more and more at off-design conditions to regulate the operating conditions. This causes flow instabilities with pressure fluctuations, and load variations that may deteriorate the machine. One effort to learn more about the flow in water turbines during transients is the Francis-99 workshops, organized at NTNU (https://www.ntnu.edu/nvks/francis-99). It is a series of three workshops, where geometrical and experimental data of a Francis turbine model is openly available for validation of CFD results. The first workshop was organized 2014, focusing on three steady operating conditions; the best efficiency point (BEP), a part load point and a high load point. The 14 papers presented at the first workshop [1] showed state-of-the art simulations of the three steady operating conditions using a wide range of CFD codes, including OpenFOAM. The second workshop was organized in 2016 and had a focus on transients between operating conditions. Most of the 10 papers presented at the workshop [2] did however not investigate the full experimental transients that were made available. The advanced investigations require dynamic meshes that both rotate the runner, using a coupling interface to the non-rotating part of the mesh, and morph the guide vane mesh due to the change in guide vane angle during the transient. Most codes and workshop participants were not ready for such simulations at the time of the workshop. The third workshop has not yet been organized. It should focus on FSI, including the deformation of the runner. That will require to also add deformation to the rotating mesh.

The present work addresses the scope of the second Francis-99 workshop, using OpenFOAM-2.3.x. The standard code has a class for dynamic mesh motion that can handle rotating regions coupled to stationary regions using the AMI interface. It also has a class for mesh morphing. Those two classes are combined in the present work, to allow simulations with both a rotating runner region and guide vanes that continuously change angle. Due to the large deformation of the guide vane mesh it is necessary to map the fields to new meshes of better quality a number of times during the procedure. Most of the meshes are generated using cfMesh, but snappyHexMesh is used when the distance between the guide vanes becomes too small. Turbulence is modelled by LES based on the dynamic one-equation eddy viscosity sub-grid model (dynOneEqEddy) [3] and the cube root volume filter width. The time term is discretized using CrankNicolson 0.5, and the convection term for velocity is discretized using linearUpwind Grad(U). The inlet and outlet boundary conditions are set using total pressure conditions. The outlet total pressure is taken from the experiment at BEP. The inlet total pressure is adjusted to yield the same flow rate as in the experiment at BEP. Those conditions are kept during the transient. We here present numerical results at BEP and when closing the guide vanes, comparing with the experimental data.

Figure 1 shows the geometry and the locations of the experimental measurements [4]. The flow enters through the spiral casing, through the stationary stay and guide vanes, through the rotating runner with full blades and splitter blades, continuing through the draft tube. A number of pressure transducers are mounted at different locations, named VL01 (Vane-Less space), VL2 (not shown in figure, but at a similar location as VL01), P42, P71 (Pressure side of runner blade), S51 (Suction side of runner blade), DT11 and DT21 (Draft Tube). DT5 and DT6 are located at similar positions as DT11 and DT21, but at different angles. It should in particular be noted that it is only the experimental data for the pressure at VL2, DT5 and DT6 that is obtained from the second workshop. The other pressure data is from the first workshop, at a slightly different operating condition. PIV measurements of the velocity distribution were made at the plane that is shown as a striped rectangle below the runner, at an angle shown with respect to the spiral casing (top view of spiral casing). Velocity distributions were extracted from the PIV data along Lines 1-3, to the extent of the PIV plane.
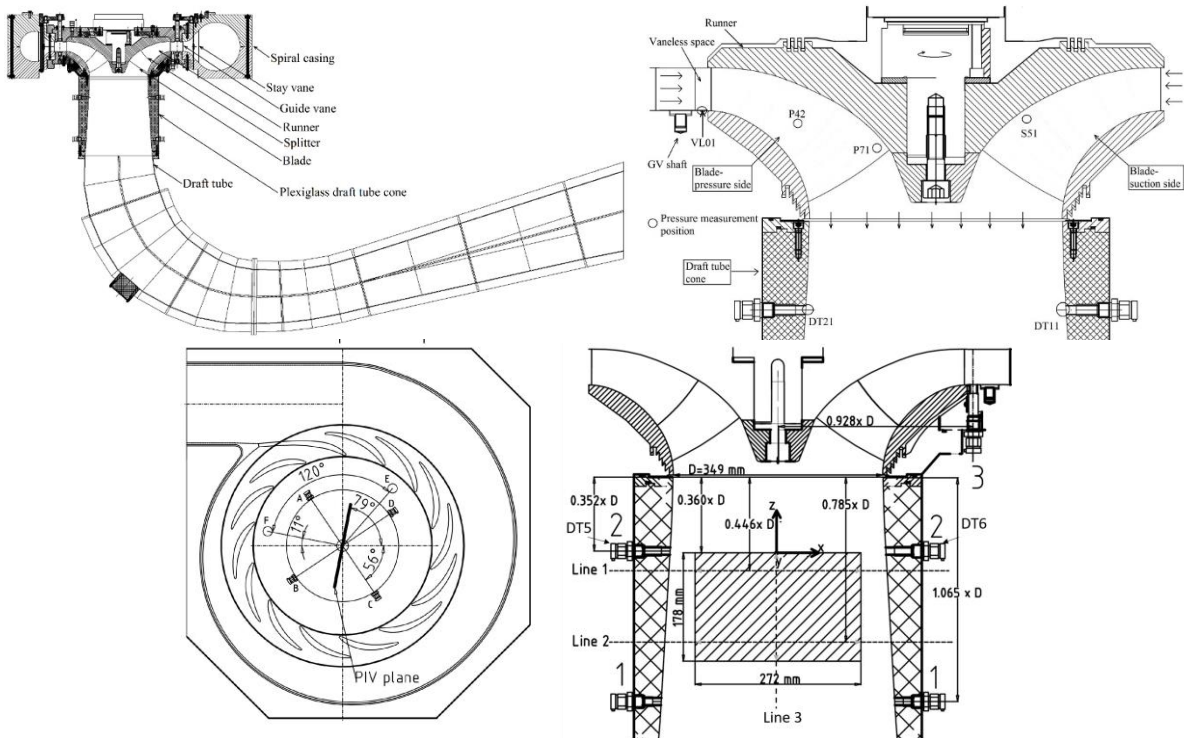
Figure 1: Geometry and locations of experimental measurements.

Figure 2 shows the mean and fluctuating experimental and numerical pressure at various probes, at the BEP operating condition. It can be seen that the mean pressure distribution through the machine is predicted qualitatively correct. It should be recalled that only the VL2 measurement was done at the same conditions as in the present simulation, which is why that point shows the best agreement. The fluctuating pressure at DT5 and DT6 show similar experimental and numerical behaviour, as well as standard deviation. The experimental data was here presented as deviation from the mean value of the sequence, as then also done for the numerical data.
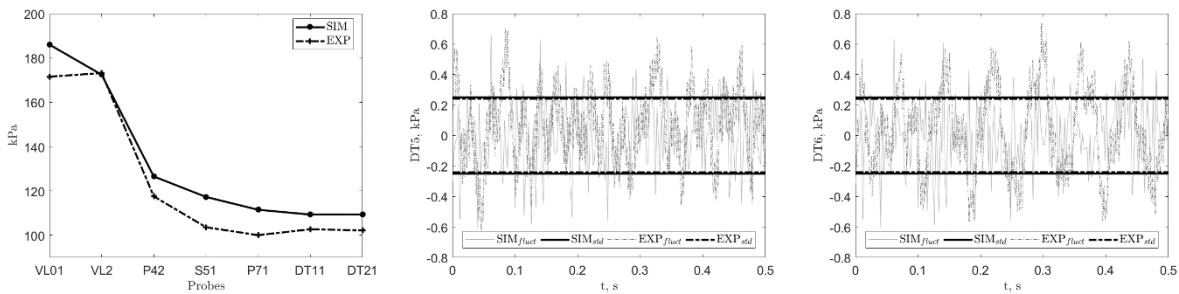

Figure 2: BEP experimental (EXP) and numerical (SIM) static pressure comparisons. Left: Mean data in various probes (see Figure 1). Center and right: Fluctuations and standard deviation at probes DT5 and DT6.

Figure 3 shows the mean axial and horizontal velocity components along Line 1, at BEP. The axial component is positive in the (0, 0, 1) direction and the horizontal component is positive in the (-0.191, -0.982, 0) direction, according to the workshop descriptions (i.e. along two perpendicular directions parallel to the PIV plane). The horizontal direction is thus a measure of the radial component, but with a change in sign at $r/R_{max}=0$. The axial component shows a very good agreement compared to the experimental data. The deviation close to $r/R_{max}=0$ is similar as for the better ones of the workshop contributions.
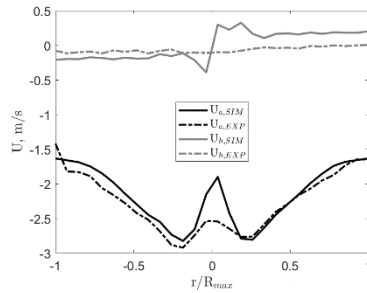
Figure 3: BEP experimental (EXP) and numerical (SIM) mean velocity profile comparisons at Line 1, where a =axial and h = horizontal. R_{max} is the largest radial position along the experimental line (i.e. extent of PIV plane, not draft tube wall).

Figure 4 shows a top view of the guide vane mesh at BEP, and while morphing it by changing the guide vane angle up to 2.6 degrees. At a 3 degree angle change it is necessary to generate a new mesh and map the fields to the new mesh in order to be able to continue the simulation. As the space between the guide vanes gets more narrow it is necessary to switch mesh and map field more frequently. In the lower part of each of the pictures it is possible to see a top view of the rotating runner mesh and the rotor-stator interface.
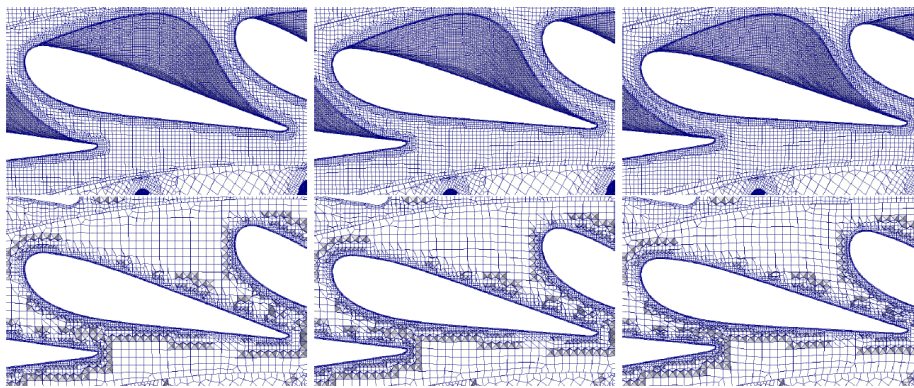

Figure 4: Guide vane mesh during a 2.6° guide vane angle change. Top: At upper cover (also showing a part of the special shape of the guide vane walls, at the densely meshed region above the guide vane). Bottom: Mid-plane. Left: 9.84° (BEP, and original mesh that the meshes at the other angels are morphed from), Center: 8.54°, Right: 7.24°

Figure 5 shows the experimental and numerical static pressure development at VL2, DT5 and DT6, as the guide vanes start closing at t=1s (at 9.84°) and change angle linearly during 7s (to 0.8°, where 0° is fully closed). The experimental data at DT5 and DT6 was presented as deviation from the mean value of each sequence, as then also done for the numerical data. It can be seen that both the general trend and the magnitude of the pressure fluctuations are similar. The major peaks in the numerical results are due to the switches between meshes.
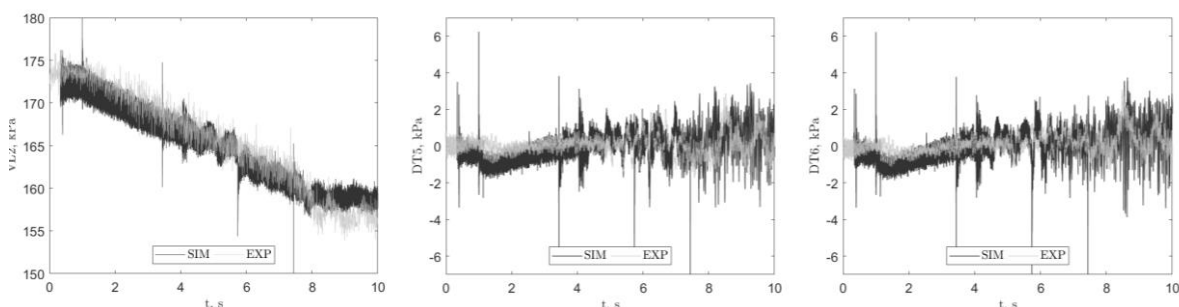

Figure 5: Transient experimental (EXP) and numerical (SIM) static pressure comparison at probes VL2 (left), DT5 (center), and DT6 (right), going from BEP and closing the guide vanes linearly from t=1s to t=8s.

Figure 6 shows contour plots of the velocity along Lines 1 and 2 during the shutdown sequence. The r/R_{max}-axis is along the measurement lines, and the t-axis is along the time (bottom to top). Both the experimental and numerical data is probed at 28 positions along the r/R_{max}-axis. The numerical data has been filtered using a filter width of 15 (using 7 time steps before and after the corresponding time step), and is presented every 50 time step to reduce the influence of the instantaneous turbulent fields. The experimental procedure must involve smoothing both in time and space, but it has not been described in detail in the Francis-99 workshop instructions.
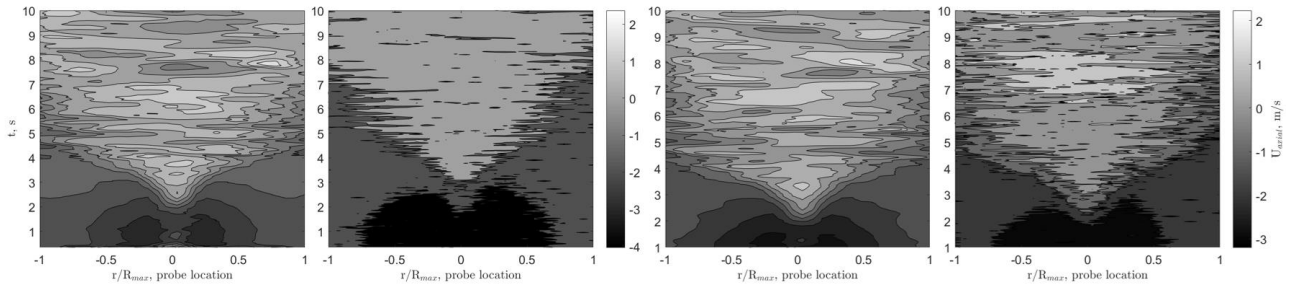
Figure 6: Velocity along line 1 (left pair) and line 2 (right pair) over time (vertical axis). In each pair, Left: simulation. Right: experiment. The guide vanes close linearly from t=1s to t=8s.

When looking at the central vortex rope using the Q-criterion one can see a significant change in flow behaviour during the transient, see Figure 7. The initial small central vortex indicates a relatively stable flow with a high axial and a moderate tangential velocity. As the velocity decreases, the flow is diverging towards the wall and the tangential velocity becomes dominant. This creates a wider vortex in the center of the draft tube that eventually breaks up in 2-3 processing vortices, which finally breaks up in several more chaotic vortices.
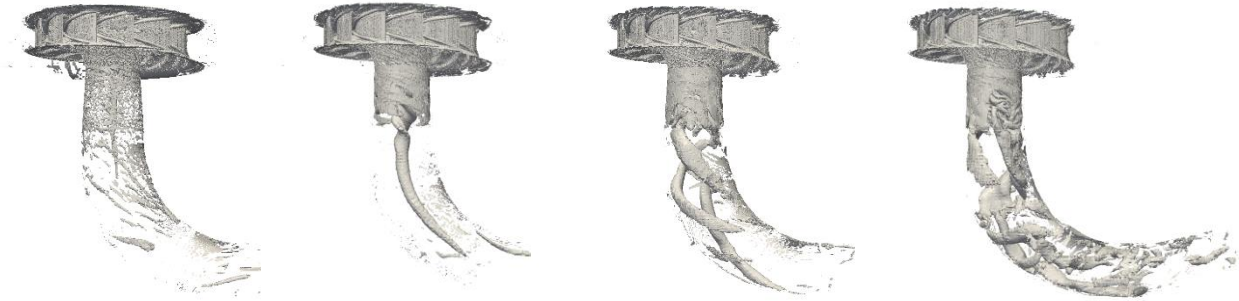

Figure 7: Iso-surface of the Q-criterion (iso-value 200). Left: BEP, at initiation of guide vane closing. Center left: guide vanes appr. 3.3° from BEP. Center right: guide vanes appr. 4.2° from BEP. Right: guide vanes appr. 6.2° from BEP.

References

[1] Cervantes, M.., Trivedi, C., Dahlhaug, O.G., Nielsen, T.K. (editors), 'Francis-99 Workshop 1: Steady operation of Francis turbines', IOP Conf. Series: Journal of Physics: Conf. Series 579 (2015) 011001, doi:10.1088/1742-6596/579/1/011001

[2] Cervantes, M.., Trivedi, C., Dahlhaug, O.G., Nielsen, T.K. (editors), 'Francis-99 Workshop 2: transient operation of Francis turbines', IOP Conf. Series: Journal of Physics: Conf. Series 782 (2017) 011001, doi:10.1088/1742-6596/782/1/011001

[3] Lillberg, E., Nilsson, P., 'Generic CFD for Vortex Induced Acoustic Resonance in Deep Cavities', ICONE16, 2008

[4] Trivedi, C., Cervantes M., Dahlhaug, O.G., 'Experimental and Numerical Studies of a High-Head Francis Turbine: A Review of the Francis-99 Test Case', Energies, vol. 9/no. 2, 2016, pp. 1-24.